The Effects of Thick Thermal Barrier Coatings on Low-Temperature Combustion

Ziming Yan, Brian Gainey, Benjamin Lawler
Clemson University

Deiva, John, Felipe, Carl, Sanjay
Stony Brook University

Abstract

An experimental study was conducted on a Ricardo Hydra single-cylinder light-duty diesel research engine. Start of Injection (SOI) timing sweeps from -350 deg aTDC to -210 deg aTDC were performed on a total number of five pistons including two baseline metal pistons and three coated pistons to investigate the effects of thick thermal barrier coatings (TBCs) on the efficiency and emissions of low-temperature combustion (LTC). A fuel with a high latent heat of vaporization, wet ethanol, was chosen to eliminate the undesired effects of thick TBCs on volumetric efficiency. Additionally, the higher surface temperatures of the TBCs can be used to help vaporize the high heat of vaporization fuel and avoid excessive wall wetting. A specialized injector with a 60° included angle was used to target the fuel spray at the surface of the coated piston. Throughout the experiments, the equivalence ratio, ϕ, was maintained constant at 0.4; the combustion phasing was consistently matched at 6.8 ± 0.4 deg aTDC. It can be concluded that the thick TBC cases achieved 1 to 2 percentage points improvement in combustion efficiency, and generally, a ~2 percentage points increase in fuel conversion efficiency. It is also noticed that applying a dense top sealing layer to the TBC further improves the UHC emissions compared to the TBC coated piston with an unsealed surface. From the heat release analysis, it can be concluded that TBC has no significant impact on the heat release process and knock intensity while matching the combustion phasing; however, it reduces the intake temperature requirement by up to 20 K. The exhaust gas temperatures were expected to increase for the TBC cases, but the expected increase in exhaust temperature was not conclusive from the results observed in this study.

Introduction

Low-temperature combustion (LTC)

Since the transportation sector consumes approximately one-third of the total energy used by the U.S. and contributes a similar fraction of CO_2 emissions, there is a strong motivation for energy-efficient transportation solutions for automotive vehicles. Accordingly, the CAFE standards for fuel economy have become more aggressive in recent years. The newest regulations on greenhouse gases, especially CO_2 emissions, require a significant efficiency improvement over traditional spark ignition (SI) engines. Meanwhile, the next EPA tailpipe emissions regulations have nearly suspended the development of diesel engines for the light-duty market in the U.S., despite their higher efficiency compared to traditional SI engines. All of these demands and regulations motivate a revolutionary advancement in the traditional automotive powertrain. There are several promising technologies and approaches to meet these new requirements; for example, the hybrid electric powertrain is an attractive option for the light-duty market. However, improvements made to the engine efficiency can benefit both conventional vehicles and hybrid electrics and there is still a considerable amount of room for improvements to the efficiency of combustion engines from a thermodynamic standpoint. One of the advanced internal combustion (IC) engine concepts is low-temperature combustion (LTC), which is intended to operate with peak temperatures between the NO_x formation and minimum CO oxidation temperatures [1],[2]. The combustion process is comparatively clean with near-zero particulate and NOx emissions, therefore only requiring an oxidation catalyst for aftertreatment, while still achieving high thermal efficiencies similar to conventional diesel combustion due to the high ratio of specific heats ($\gamma = c_p/c_v$) associated with low temperatures and lean operation [3]. Several advanced low-temperature combustion modes have been proposed; for example, the early attempts of homogeneous charge compression ignition (HCCI) revealed its high efficiency and ultra-low emissions characteristics [4] [5]. However, the lack of control over the start and the rate of combustion limit HCCI's commercial potential [6]. Second generation advanced combustion modes like gasoline compression ignition (GCI) [7][8], partial fuel stratification (PFS) [9],[10], reactivity controlled compression ignition (RCCI) [11][12], and thermally stratified compression ignition (TSCI) [13][14] provide the means of stratifying either the equivalence ratio (ϕ), in-cylinder reactivity, or temperature distributions to allow the combustion process in LTC to be well controlled.

However, among all of the LTC modes, there is a unique challenge compared to the traditional combustion modes, SI and conventional diesel, which is the lower combustion efficiency. In LTC, the charge is overall lean and the peak bulk temperature is low, especially at lower load conditions [15]. Flowers et al. have shown that the combustion efficiency improves substantially with the intake charge heating, but the penalty is faster heat release rates and a decreased high load limit [16]. Additionally, the authors have previously shown that applying a certain amount of EGR helps improve combustion efficiency at a low-to-medium loads but could also cause deterioration in combustion if the EGR increases beyond a certain limit [17][18]. The same study also indicated that EGR changes the mixture's properties, such as its γ, which potentially decreases the amount of work that could be extracted from the engine cycle and decreases the indicated thermal efficiency. Moreover, with some second generation, controlled LTC modes such as PFS or RCCI, EGR lowers the oxygen availability and restricts the maximum load limit [19]. By understanding the sources of unburned hydrocarbon (UHC), oxygenated hydrocarbon (OHC), and carbon monoxide (CO) emissions, the combustion efficiency can be improved. Therefore, Aceves et al. investigated the geometrical distribution of the emissions by using a KIVA multi-zone model [20]. Figure 1 shows the motoring in-cylinder temperature distribution at top dead center (TDC). As can be seen, the top ring land is the coldest region and some cold regions exist near the liner and surface of the piston. These regions most likely would not reach autoignition and therefore, they contribute to incomplete combustion emissions.

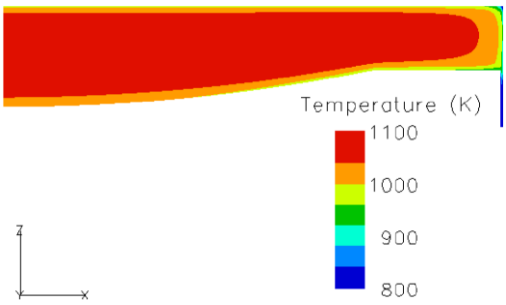

Figure 1: Simulated temperature distribution at TDC from Aceves et al. [20]

The incomplete combustion emissions can be improved by applying a layer of thermal barrier coating (TBC) onto the combustion chamber surfaces to increase their temperature and help oxidize the unburned fuel near the combustion chamber walls. However, the benefits that can be achieved by means of implementing TBCs in IC engines are not only limited to improve the combustion efficiency; TBC can also raise the thermal efficiency by reducing heat transfer and increase the exhaust gas enthalpy. A thorough introduction to TBCs is included below.

Background: Thick thermal barrier coatings (TBCs)

The concept of the "adiabatic engine" was first proposed in the early 1970s and followed by simulation studies to predict the performance by Kamo et al. [21] and Sudhakar [22]. Both studies predicted the significant potential to decrease fuel consumption and hydrocarbon emissions. Further experimental investigations were fulfilled by the Cummins/TACOM adiabatic engine program during the 1980s [23]. By the end of the program, the feasibility of utilizing TBCs on a turbocompound diesel engine was demonstrated; however, experimental testing did not show an improvement in fuel economy. It was speculated that a sufficient thickness of 5mm is required to achieve a meaningful amount of engine efficiency improvement (5% reduction in fuel consumption), and also indicated that the high surface temperatures reduced volumetric efficiency, which is one of the drawbacks of thick TBCs. Several critical challenges were listed, including high-temperature lubrication, better ceramic materials, and thickness limitation by the plasma spray application technology. However, the recent consensus is that thick TBCs are not preferred in traditional SI engines due to the high intake charge heating penalty and increased the propensity to knock [24].

Background: Thin, "Temperature-Swing" TBCs

Contrary to the thick TBC approach which results in high temperatures throughout the entire engine cycle, a new approach has been proposed that uses thin coatings to produce a "temperature swing", where the temperature of the surface fluctuates over the engine cycle. This approach solves the intake charge heating issue of thick TBC during the gas exchange phase, while providing the heat transfer insulation during the closed portion of the cycle where most of the heat transfer losses occur [25][26]. It was proven that thin TBCs for SI is a very promising approach, especially at a part load conditions, and can result in a 10% reduction in fuel consumption without the observation of engine knock/preignition [27]. The TBC surface finish is also essential. Hoffman showed that the porosity and surface roughness are speculated to be responsible for incomplete combustion and combustion chamber deposit (CCD) formation, which provides the motivation for improving the surface finish.

A considerable amount of work was conducted on traditional SI or conventional diesel combustion. More recently, initial assessments of TBCs on advanced LTC modes have been conducted. A 150 microns atmospheric plasma spray (APS) yttria-stabilized zirconia (YSZ) coating was tested and compared to a baseline metal piston under HCCI operating conditions, showing improved engine efficiency and reduced UHC and CO emissions [28]. It was also shown that compared to the aluminum piston, the operating range of a Magnesium Zirconated (MgZr) coated piston was significantly shifted downwards for both the high and low load limits, and the overall range was increased by 31% [29].

Objective of the Current Approach

In summary, the majority of the current focus is related to thin, temperature-swing TBCs for conventional combustion modes to avoid the issues of charge heating which lowers the density of the incoming air and increases the propensity to knock in SI. However, many advanced combustion concepts use high intake valve closing (IVC) temperatures by either heating the intake or intentionally trapping internal hot residuals to achieve autoignition. Therefore, these strategies could benefit from thick TBCs, which would reduce heat transfer losses and increase efficiency without imposing any additional penalty on the incoming charge density beyond the current approaches of intake heating or internal residuals. Furthermore, some recent attempts with HCCI fueled by wet ethanol have demonstrated the significant cooling potential of the intake stroke injection [30]. In fact, the fuel has such a high latent heat of vaporization (HOF), along with a high resistance to autoignition, that the intake temperature requirement can be very high, and the combustion efficiency can be low due to wall wetting and the difficulty associated with evaporating the liquid droplets. Therefore, there is the potential for a perfect marriage between thick TBCs and intake stroke injections of a high heat of vaporization fuel. It is anticipated that pairing a thick TBC with a high HOF fuel will have the following benefits:

- Reduced heat transfer losses and higher efficiencies
- Improved combustion efficiency due to higher surface temperatures
- Higher exhaust temperatures to aid LTC aftertreatment and turbocharger performance
- Lower and more realistic intake temperature requirements to achieve autoignition
- No additional charge heating penalty

Background: Wet Ethanol

Wet ethanol refers to a mixture of ethanol and water, also known as "hydrous ethanol". The current corn ethanol technology makes ethanol one of the most widely used biofuels (mass-produced at scale) in the United States [31]. The energy required and the associated cost in this corn ethanol process is exceedingly sensitive to the water content in ethanol due to the distillation and dehydration processes. Many studies have shown that removing the water content in ethanol consumes an enormous amount of energy during the ethanol production process [32], and the energy consumption is highly nonlinear as the ethanol percentage exceeds ~80%. An illustration of the energy consumption during the fermentation, distillation, and dehydration is shown in Figure 2, which is based on data presented in [33]. Therefore, wet ethanol containing 20% or more water presents a quite attractive option: to bring down the cost and energy consumption associated with the production of biofuel while absorbing CO_2 emissions during the production of a renewable fuel that is scalable.

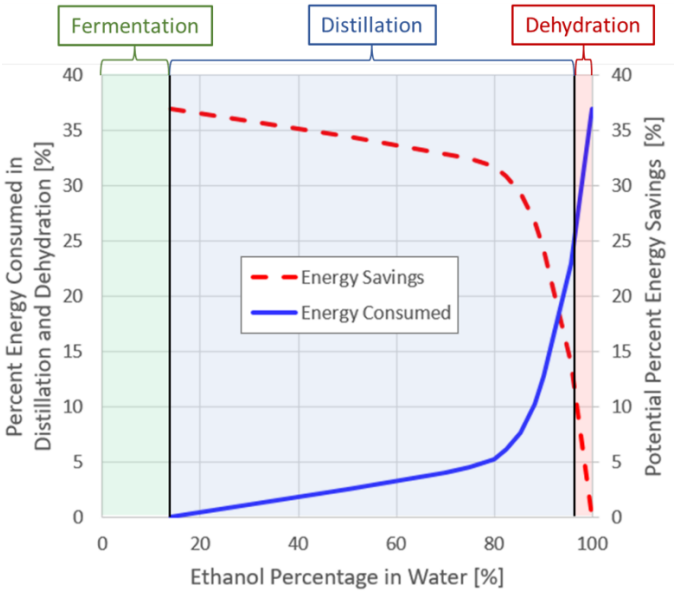

Figure 2: Energy required to remove the water content from ethanol.

Beyond the production benefits of leaving some water content in the ethanol, the fact that wet ethanol has an excellent cooling potential makes it ideally suited to address the normal charge heating penalty associated with thick TBCs. This is the motivation for this study:

To assess the effects of thick TBCs on advanced low temperature combustion enabled by a fuel with a high latent heat vaporization.

Experimental Setup and Methodology

The experimental setup and methodology are divided into two sperate sections. The first section includes the introduction to the engine test cell and combustion analysis. The second section introduces the plasma thermal spray technology as well as the properties of the coating.

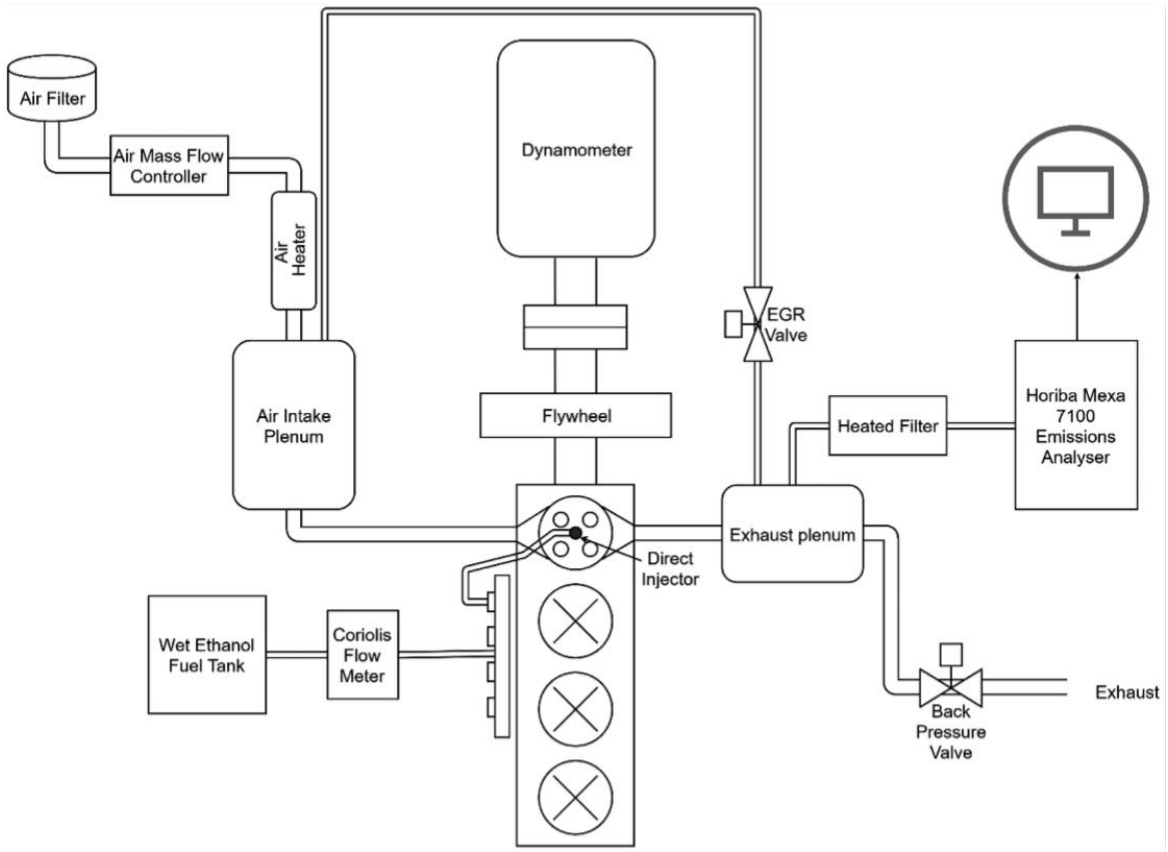

Figure 3: Engine test cell layout

Experimental engine test cell

A 0.4215-liter single-cylinder light-duty diesel engine was used to conduct the experiments. Figure 3 is a schematic of the complete engine system. The first cylinder of a production four-cylinder, 1.7-liter GM-Isuzu engine head is coupled with a Ricardo Hydra research engine block, and the other cylinders are deactivated. In favor of improving the incomplete combustion and the unburned hydrocarbon emissions associated with LTC, a custom-designed shallow bowl piston was utilized to substitute the traditional OEM re-entrant diesel bowl piston. The geometry of the combustion chamber at the TDC is shown in Figure 4. It can be observed that the squish region has been substantially reduced while maintaining the same compression ratio (CR). Additionally, the heat transfer losses can be reduced due to a more beneficial surface-to-volume ratio [34].

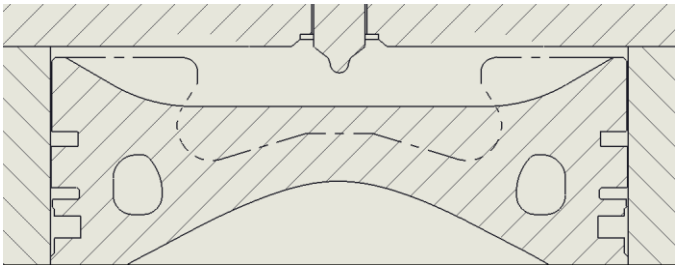

Figure 4: Geometry of the combustion chamber at TDC

Table 1: Engine specifications

Displaced volume	421.5 cc
Stroke	86 mm
Bore	79 mm
Connecting Rod	160 mm
Compression ratio	Targeted at 15.8:1
Number of Valves	4
Exhaust Valve Open	140° ATDC
Inlet Valve Close	-146° ATDC

Some of the relevant engine specifications are shown in Table 1. In the process of machining several pistons to be tested, some with and some without TBCs applied, there were slight errors in the clearance volume caused by the machining process that caused the compression ratio to deviate from the targeted value of 15.8:1. The compression ratios of the coated pistons varied slightly from 14.7 to 15.2. Figure 5 shows the piston preparation process from the unmachined blank piston to the final coated piston with the desired shallow bowl shape. First, the blank piston was machined down to the different levels with shallow bowl shape depending on the desired TBC thickness. Then, the primary coating materials were plasma sprayed onto the top surface of the piston, layer-by-layer, while masking the other piston surfaces such as the ring pack area and the piston shirt. The last step is to create a dense sealing layer on the top surface of the coating, if desired, which involved spraying a much denser layer of smaller particles of the same material onto the surface of the coated piston. The TBC surface was finished with some light polishing of the ceramic surface. The detailed coatings techniques will be introduced in the following sections.

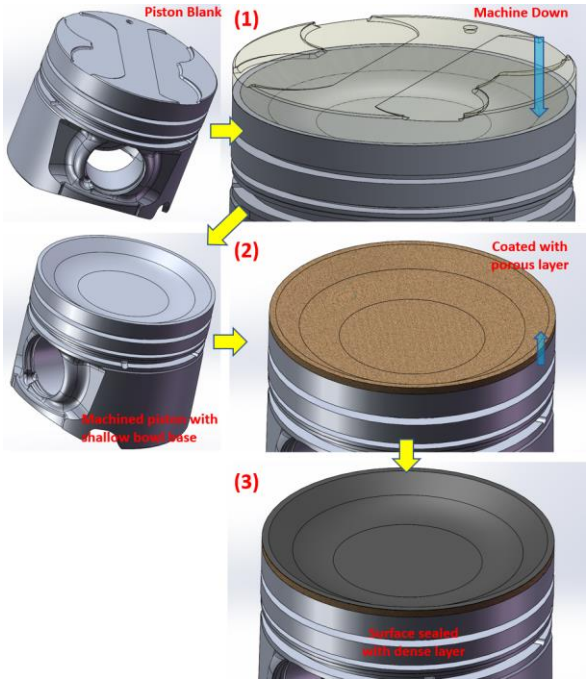

Figure 5: TBC machine & spray process

In this study, the performance of three coated pistons are compared to two uncoated metal pistons. The coated pistons include two pistons with a 1mm and a 2mm coating that are finished by the surface sealing process, and a 2mm coated piston without the surface sealing.

The fuel selected in this study is wet ethanol, which is made from a mixture of 80% ethanol and 20% water on a mass basis. The fuel system was from a conventional diesel engine fuel delivery system using the high-pressure common rail with a Bosch CP3 pump and a Bosch solenoid-style direct injector. Based on the combustion mode and start of injection (SOI) timings, a centrally mounted six-hole injector tip (DLLA60P) with a 60° included angle was used. This injection angle allows the spray to target the piston surface to avoid creating excessive wall wetting and impingement on the cylinder liner and the crevice volumes. Since wet ethanol does not have the same lubricative ability as diesel, 500 ppm of Infineum R655 lubricity additive was premixed with the wet ethanol before adding the fuel to the fuel system. Previous experimental test results showed that adding this amount of lubricity additive does not have a noticeable impact on the fuel's autoignition properties or the combustion process [35].

Because wet ethanol has a very high latent heat of vaporization and results in a high intake temperature requirement to achieve autoignition in HCCI, a 5-kW intake heater is located upstream of the intake plenum and is PID-controlled via a custom Labview program to precisely control the intake temperature. The exhaust gases are sampled from the exhaust plenum and delivered to a Horiba MEXA 7100 D-EGR emissions analyzer through a heated filter and sample lines. Six specific emissions are measured, which are UHC, CO, CO_2, O_2, and oxides of nitrogen (NO_x). The intake pressure and cylinder pressure are measured based on a high-speed basis, which is triggered by a Kistler 2614C11 crank angle encoder at a resolution of 0.1 crank angle degree (CAD).

All of the acquired data mentioned above are monitored and recorded through the Labview program. Some of the combustion performance characteristics, such as indicated mean effective pressure (IMEP),

efficiencies, and heat release profile are calculated in real-time and shown during operation. Once the combustion reaches steady-state, 300 consecutive cycles of data were saved and further analyzed with a high-fidelity Matlab script that uses the NASA polynomials for mixture properties and uses a heat transfer correlation for to calculate the gross heat release rate.

The table below shows the engine operating conditions. All of the experiments in this study were conducted under naturally aspirated conditions at an engine speed of 1200 rpm without EGR.

Table 2: Engine operating conditions

Engine Speed [rpm]	1200
DI Fuel	Wet Ethanol 80
DI SOI Timing [deg aTDC]	Swept from -350 to -210
DI Pressure [bar]	500
IMEPg [bar]	3.8
Coolant Temperature [K]	370
Oil Temperature [K]	360
Equivalence ratio, ϕ	0.4
Combustion Phasing- CA50 [deg aTDC]	6.8

The variation of CA50 for all of the data collected is less than half of a crank angle degree, the variation of intake temperature is less than 0.3 K, and the coefficient of variation (COV) of net IMEP is less than 3%. For safety considerations, the peak pressure rise rate (PPRR) is maintained under 6 bar/CAD.

Application of TBCs and thermophysical measurements

All of the thermal barriers were fabricated using an argon-hydrogen atmospheric plasma spray process (Oerlikon Metco, F4MB) configured with a 6mm nozzle and a 90° 1.8mm injector and were composed of 4-5 layers depending on whether sealing was included. Carrier gas flow rates were optimized on a per-run basis using principles reported by Vasudevan et al. [36], while plasma gas flow rates and power were optimized based on a two-level three factor central composite design of experiment based on in flight particle properties (Tecnar Automation AccuraSpray 3G) as described by Vaidya et al. [37], with relevant data tabulated below.

Table 3: APS configurations

Layer	L1	L2	L3	L4	L5
Argon [NLPM]	45	45	45	45	47
Hydrogen [NLPM]	4	6	6	6	6
Current [A]	550	550	550	550	600
Carrier Gas [NLPM]	3.5	4	3	3.5	3.5
Spray Distance [mm]	100	150	150	150	100

Coatings on the millimeter scale have been historically prone to cracking, delamination, or other failures induced by thermal stresses during the engine cycle [38]. These thermal stresses are generally a function of the difference between the thermal expansion of the coating and the base material, the coatings compliance and thickness, and the temperature history over the thickness of the coating [39]. As such, grading the coefficient of thermal expansion (CTE) through the plasma spray process has been previously established as a successful control scheme for mitigating thermal stresses [40] [41]. This was accomplished by varying the coatings composition from pure Ni5Al (Oerlikon Metco, 480NS) at the coating-base material interface to a 95-5% mixture by volume of yttria-stabilized zirconia (Saint Gobain, SG204) and Ni5Al respectively on the free surface in a series of discreetly sprayed layers that form a smooth grading.

Before coating the pistons, their surfaces were prepared by grit blasting at 60 psi from a 125mm distance using 24 mesh alumina grit, followed by the removal of entrained grit and organics by isopropyl alcohol then rinsed in purified deionized water and dried with compressed air. All pistons were first coated with a Ni5Al bond coat layer representing 5% of the total coating thickness that, in addition to mediating thermal expansion, increases adhesion strength and resists high-temperature oxidation. Next, a 50-50% by volume YSZ-Ni5Al layer representing 10% of the total thickness was applied, followed by a 70-30% by volume layer representing 20% of the total thickness, and finally a 95-5% by volume layer representing 65% of the total thickness, with an additional thin 97-3% by volume sealing layer. A finer YSZ feed stock (Saint Gobain, SG240F) was used in the fabrication of the sealing layer as well as a finer Ni5Al (Orelikon Metco, Diamalloy 4008).

The thermophysical properties of each layer, as well as the composite coating, were measured using a thermal flash method (TA Instruments DXF 3050) and the Clarke-Taylor approximation for radiative and convective heat losses as well as finite pulse width corrections per ASTM E1461 standards. In this method, thermal conductivity is calculated as the product of diffusivity, density, and specific heat using the simultaneous measurement of thermal diffusivity and specific heat and density measured by the Archimedes principle. A summary of coating layer thicknesses and thermophysical properties are given below with k, ρ, c, and α representing the thermal conductivity, density, specific heat, and thermal diffusivity of each layer. Figure 6 shows a scanning electron microscope (SEM) image of the unsealed and sealed TBCs layers after being applied to the piston surface.

Table 4:Coating layer properties

Layer	L1	L2	L3	L4	L5
1mm Layer Thicknesses [μm]	50	100	200	650	40
2mm Layer Thicknesses [μm]	120	240	480	1560	40
2mm Unsealed Layer Thicknesses [μm]	120	240	480	1560	-
k [$Wm\text{-}1K^{-1}$]	14.23	7.57	4.48	0.93	1.74
α [cm^2s^{-1}]	0.0462	0.0415	0.0252	0.0052	0.0069
ρ [kgm^{-3}]	7511	5893	5577	4490	5706
c [$kJkg^{-1}K^{-1}$]	410.3	309.2	318.9	362.8	441.5

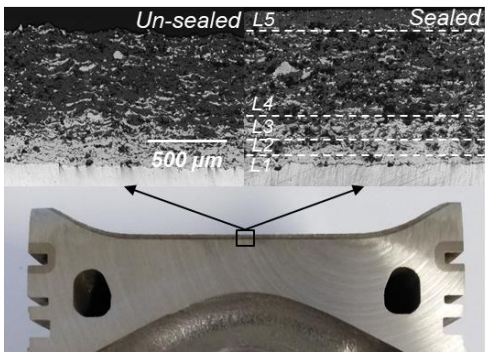

Figure 6: SEM picture for TBCs layer

Result and Discussion

In this study, three coated pistons with either different coating thickness (1 mm and 2 mm) or different surface finishes (sealed with a thin, dense layer of the same material or unsealed) are compared to the two metal pistons as the baselines. Since the exact compression ratio of each machined piston varied slightly, two metal baselines were tested to bracket the coated pistons in terms of their compression ratios. The first metal baseline configuration used a thin head gasket, which provided a CR of 15.8:1. The second metal baseline used a thick head gasket that resulted in a larger clearance volume and lower CR. The relationship between peak motoring pressure and intake temperature for these coated pistons and baselines are shown in the figure below. The figure shows that the metal piston with the thick head gasket had the lowest CR of 14:1, and the same piston with the thin head gasket had the highest CR of 15.8:1. All of the coated pistons are located between the baseline metal piston cases and are relatively close to each other in terms of their compression ratios. The coated pistons have comparable compression ratios ranging from 14.7:1 to 15.2:1. Ideally, the compression ratios of each piston would be matched perfectly experimentally. However, due to very slight machining inaccuracies, it was not possible to perfectly match the compression ratio. Instead, the two metal baseline cases bracket the TBC cases. Therefore, when the results for any of the TBCs fall outside of the bracketed range of the baseline metal cases, it can be concluded that the effect of the TBC was strong enough to overcome the differences in the compression ratio. In this way, despite the slight differences in the compression ratio between the TBC cases and the metal baseline cases, a fair comparison can still be made. Since the compression ratio discrepancy between the TBC cases is minimal, these cases can be compared directly. The peak motoring pressure (as an indicator of combustion ratio) versus intake temperature is shown in the figure below.

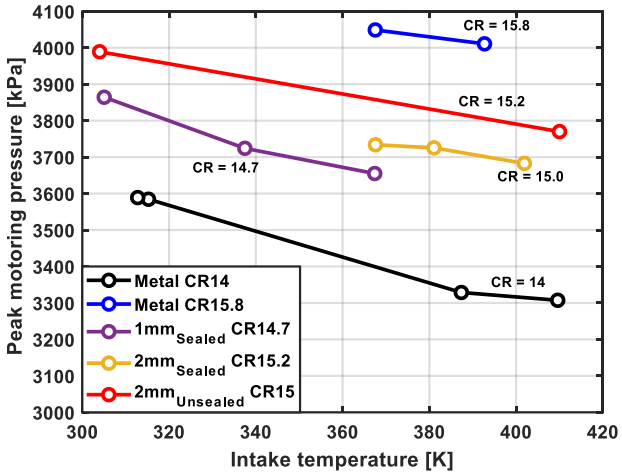

Figure 7: Peak motoring pressure vs. intake temperature for the different tested piston

This study mainly focuses on the effect of thick TBCs on the performance characteristics of combustion and the heat release process. Since wet ethanol has a high latent heat of vaporization, a sweep of SOI timing from -350 to -210 deg aTDC is used to help study the effects of thick TBC with a high heat of vaporization fuel in advanced combustion.

The heat release process

It can be observed in Figure 8 that all of the cases have very similar heat release characteristics. Additional gross heat release rate (GHRR) plots for other SOI timings are provided in the Appendix, Figure 14. Other heat release indicators, such as peak pressure rise rate (PPRR), CA50, and burn duration for all SOI timings, are shown in Figure 9.

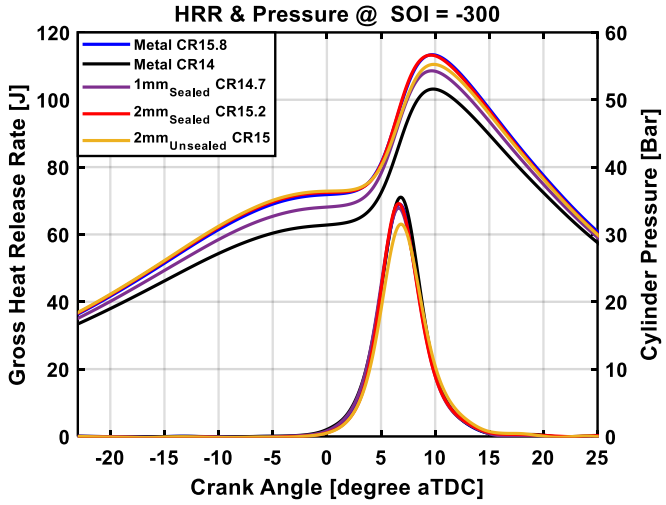

Figure 8: Gross heat release rates (bottom) and pressure traces (top) vs. crank angle degree at SOI of -300 deg aTDC

The CA50s are targeted at a constant phasing around 6.8 deg aTDC, by adjusting the intake temperature, which is shown in Figure 9(b). The metal piston with the thick head gasket has a narrower SOI timing sweep (truncated at -250 deg aTDC), due to the high intake temperature requirement for the low compression ratio case. The maximum intake temperature supported by the experimental setup is 470 K, which was reached, and the injection timing could not be retarded further. For all cases, the PPRR has a generally consistent agreement. Although the 2mm sealed TBC case is usually slightly higher than the others, the TBCs generally did not increase the pressure rise rate noticeably, despite the higher piston surface temperature. By examining all of the cases in Figure 9 and the GHRR figures in the Appendix, it can be concluded that TBC did not significantly impact the heat release process and the knock intensity when matching CA50.

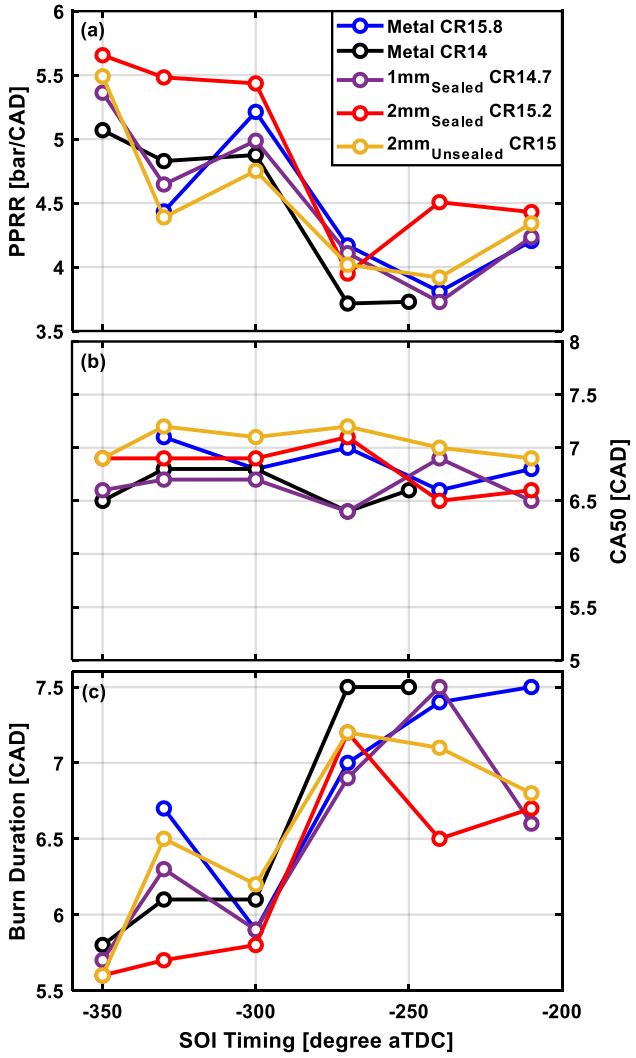

Figure 9: (a) PPRR, (b) combustion phasing, (c) burn duration vs. SOI timing with different coated pistons and the metal baseline cases

Efficiencies and Emissions

The efficiency terminology used in this study follows the definitions from Heywood [3]. The *combustion efficiency*, η_{comb}, is the percent of fuel that burned, and it is determined from the emissions based on the percentage of each emissions constituent. Then, the *gross indicated fuel conversion efficiency*, $\eta_{ig,fuel}$, is the gross efficiency of the engine based on the total amount of fuel being supplied to the engine. The mathematical definition of $\eta_{ig,fuel}$ is provided in Equation (1), where the W_{ig} is the gross work from the pressure-volume calculation, m_{fuel} is the total mass of fuel injected into the cylinder each engine cycle, and Q_{lhv} is the lower heating value of the fuel.

$$\eta_{f,ig} = \frac{W_{ig}}{m_{fuel} * Q_{lhv}} \quad (1)$$

In order to investigate the efficiency from a thermodynamic standpoint and to decouple the effect of unburned fuel, the *gross indicated thermal efficiency*, $\eta_{th,ig}$, is introduced. This efficiency only considers the energy added to the thermodynamic cycle, i.e., the energy released from the fuel that burned, not including the lost energy from incomplete combustion. The relationship between these three efficiencies are shown in Equation (2)

$$\eta_{ig,th} = \frac{W_{ig}}{m_{fuel} * Q_{lhv} * \eta_{comb}} = \frac{\eta_{f,ig}}{\eta_{comb}} \quad (2)$$

Figure 10 shows the effects of different TBCs on (a) combustion efficiency, (b) gross indicated thermal efficiency, and (c) gross fuel conversion efficiency.

It can be observed from Figure 10(a) that the two metal piston baseline cases are relatively close to each other, and the thick head gasket (lower CR) case has a slightly higher combustion efficiency. That is most likely due to the reduced compression ratio, which lowers the pressure before combustion and reduces the portion of mass trapped in the crevice volume after compression. This result is in good agreement with the findings of Dec et al. who documented a similar increase in combustion efficiency with a decrease in CR [42]. Compared to the baseline cases, all of the TBC cases display a noticeable improvement in combustion efficiency by up to two percentage points. The 2mm sealed case has the highest combustion efficiency among all of the tested pistons. The 1mm sealed and the 2mm unsealed cases are very similar, which are slightly lower than the 2mm sealed case, but higher than the metal baseline cases for most of the injection timings. This combustion efficiency improvement is presumably due to the higher surface temperatures enabled by applying a thick TBC. The hotter piston surface raises the temperatures of the cold regions near the piston, where the UHC and CO oxidation is typically challenging. The improved combustion efficiency indicates that the effect of the thick TBCs on combustion efficiency overpowers the effect of compression ratio on combustion efficiency.

Additionally, a comparison can be made between the 2mm sealed coating and the 2mm unsealed coating, where the sealed coating displayed a higher combustion efficiency. This is most likely due to the open pores and surface roughness of the unsealed TBC storing unburned fuel. With the sealed and polished surface, the combustion efficiency is noticeably higher suggesting that some form of top sealing of the TBC to reduce open porosity and surface roughness is beneficial for improving the combustion efficiency in advanced combustion concepts. Other researchers have also explored surface roughness or top seal coats and noticed similar favorable results [43].

The combustion efficiency generally increases with SOI timing before -270/-240 deg aTDC, then decreases. The reason for this trend is that at early SOI timings such as -350 to -330 aTDC, the piston is very close to TDC, and there is not much air in the cylinder yet. Therefore, the fuel impinges upon the piston surface, which results in some mass in the wall film and lowers the combustion efficiency. As the piston moves down at later SOI timings around -270/240 deg aTDC, a considerable amount of hot air is inducted into the cylinder, which helps spray break up and provides heat to compensate for the evaporative cooling. Therefore, the unburned fuel decreases due to less mass in the wall film and the combustion efficiency increases. As the injection timing is delayed further, the combustion efficiency starts to decrease after -240 deg aTDC due to the spray targeting the crevice volume around -230 deg aTDC, where the unburned fuel is stored and released as a significant portion of UHC emissions. Further delaying injection timing leads to the fuel spray impinging upon the cylinder liner which causes wall wetting and lowers combustion efficiency. Figure 11 includes a 3D CAD model that shows the spray angle and piston position at different injection timings, which supports the

explanations above. Additionally, the trends in air mass flow shown in Figure 13(a) also support the theory explained above.

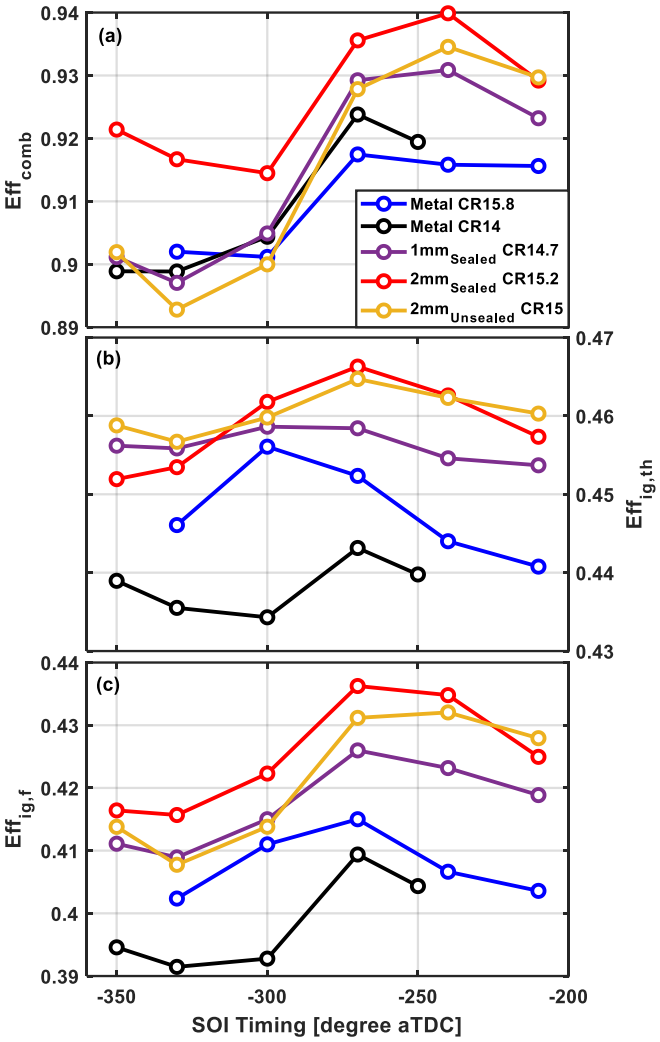

Figure 10: Efficiencies vs. SOI timing for the different coated and metal baseline pistons

The gross indicated thermal efficiency is shown in Figure 10(b). The metal baseline with the thick head gasket has a lower efficiency than the metal baseline with the thin gasket, which is due to the reduced compression ratio. When comparing the metal baseline cases to the thick TBC cases, the efficiency is noticeably higher with the thick TBCs applied to the piston. Furthermore, the efficiency increases with the TBC thickness because of the higher surface temperatures and the reduction in heat transfer losses. Again, even with a reduced compression ratio, the gross indicated thermal efficiency of the TBC cases is still higher than the metal baseline with the thin head gasket, which proves the effectiveness of TBCs at reducing heat transfer losses and improving thermal efficiency. The fuel conversion efficiency can be determined by multiplying the combustion efficiency and the gross indicated thermal efficiency. It can be seen in Figure 10(c) that the TBC with the 2mm sealed coating achieves the highest fuel conversion efficiency. Compared to the metal baseline cases, the overall improvement in fuel conversion efficiency is about two percentage points, which is a combined result from improved combustion efficiency and the increased gross indicated thermal efficiency due to lower heat transfer losses.

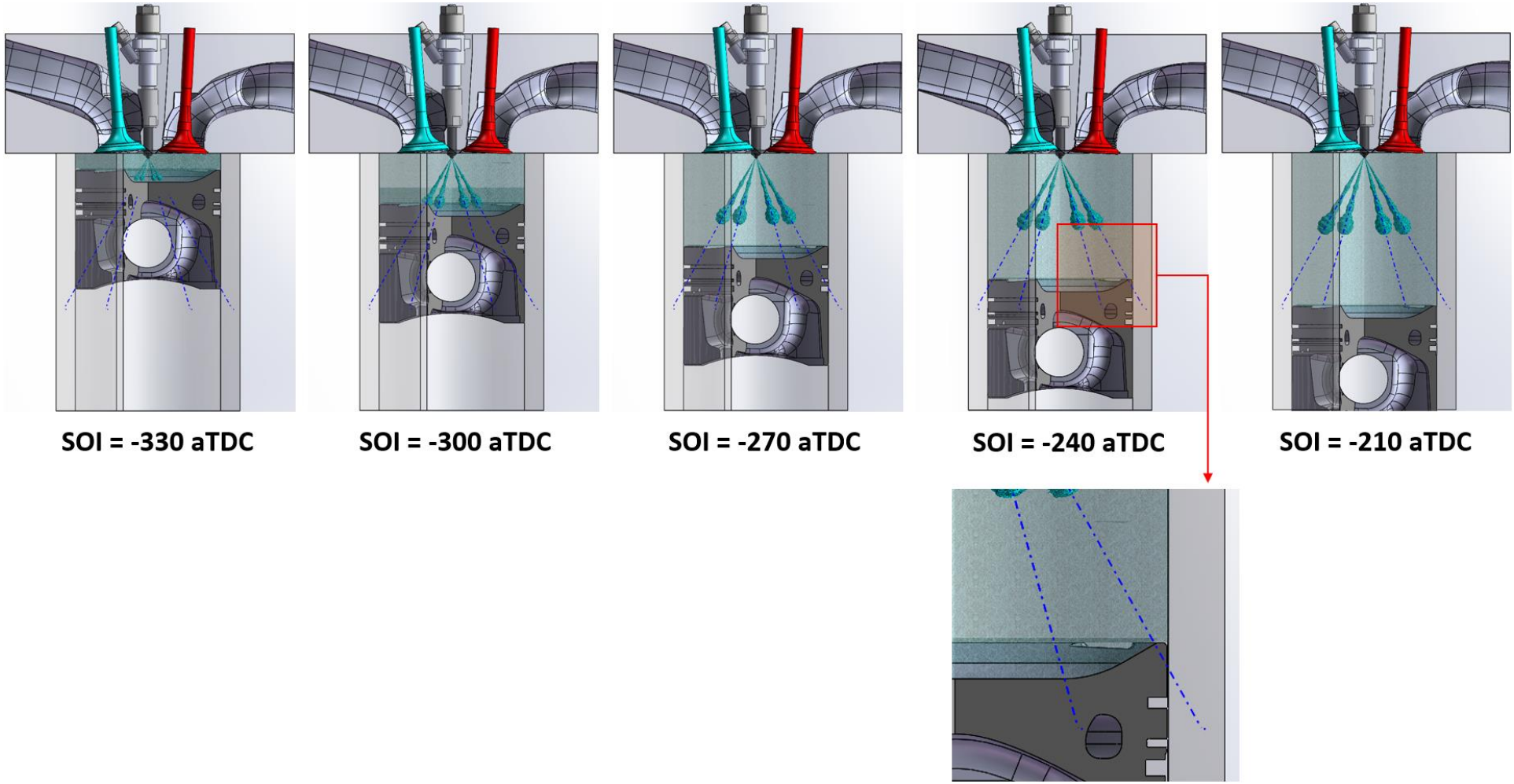

Figure 11: Fuel spray visualizations at injection timings of -330, -300, -270, -240, and -210 degrees aTDC

Figure 12 shows the estimated peak cylinder temperature and emissions with different coated pistons and the metal baseline cases. The UHC and CO emissions trends agree well with the trend in combustion efficiency discussed above. Both the UHC and CO emissions decrease with TBC cases due to an increased piston surface temperature. It is interesting to note that the increase in combustion efficiency was not only due to a decrease in UHC emissions, but that the CO emissions also decreased with the TBCs. Since the charge can be considered as a nearly homogenous mixture, the NOx emissions are related to the peak cylinder temperatures. The temperatures for most of the cases tested in this study are low enough to avoid excessive NO_x formation and the NO_x emissions remain at a very low level. The TBCs did not affect the overall NO_x emissions at these conditions and for this advanced combustion mode.

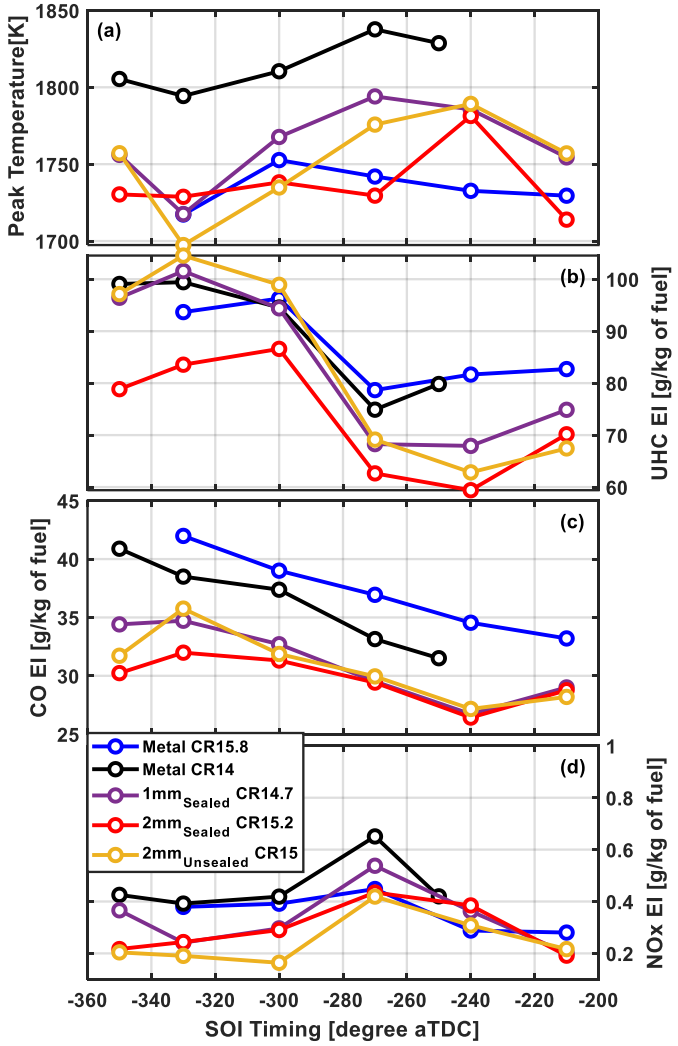

Figure 12: Emissions and peak cylinder temperature vs. SOI timing for the different coated and metal baseline pistons

The intake and exhaust temperatures

The intake temperature and exhaust temperature are shown in Figure 13 (a) and (b), respectively. It can be concluded by comparing the two metal piston baselines that the intake temperature requirement is higher with a reduced compression ratio, which is consistent with the literature and intuition about advanced combustion. However, all of the TBCs have a lower compression ratio compared to the metal piston with the thin head gasket, and the two 2mm coated piston have the lowest intake temperature requirement. This reduced intake temperature requirement is due to the hotter surface with the TBC pistons compared to the metal piston due to the insulating effect of the coating. As a result, the incoming air is heated more by the coated piston surface than the bare metal surface. This is the charge heating effect that is detrimental to conventional combustion modes because it decreases charge density and can lead to knock in SI combustion. However, in advanced combustion, the IVC temperature is usually elevated by high intake temperatures or by internal residuals to achieve autoignition. Therefore, there is no additional penalty of applying thick thermal barrier coatings to advanced combustion because there is no decrease in density beyond what would already be experienced; there is only the significant benefit to thermal efficiency and combustion efficiency.

The exhaust temperatures for TBC cases were expected to be higher than the metal baseline cases due to the lower heat transfer losses from the better-insulated combustion chamber. Some of the would-be heat transfer losses were converted to work, which is why the thermal efficiency increased, and some of that saved energy is rejected to the exhaust. However, there is no observable effect of the TBCs on the exhaust gas temperature from this experimental study, possibly due to the compression ratio differences, or possibly due to experimental inaccuracies in measuring the exhaust temperature. There are also no observable changes in exhaust temperature with delayed injection timings.

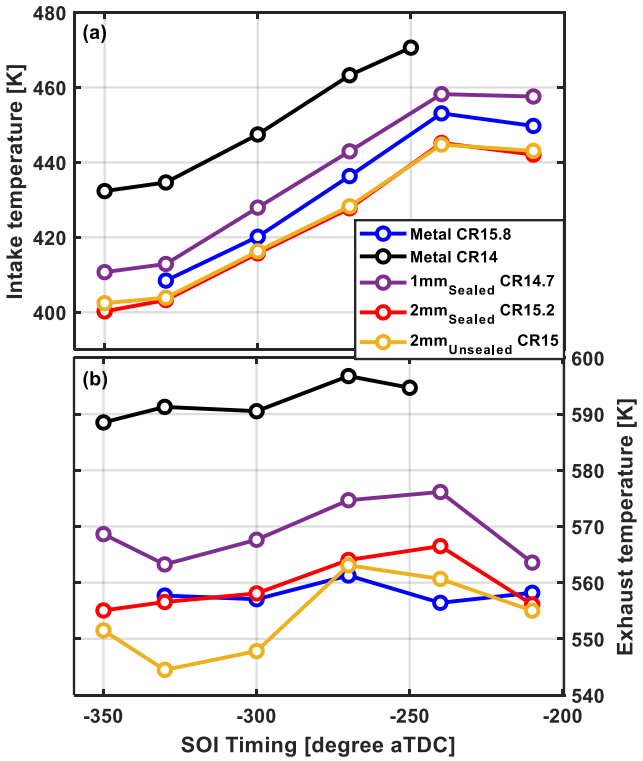

Figure 13: The intake temperature requirements and the measured exhaust temperatures vs. SOI timing for the different coated and metal baseline pistons

Conclusions

An experimental study was conducted on a Ricardo Hydra single-cylinder light-duty diesel engine. SOI timing sweeps were performed on a total number of five different pistons to investigate the effects of thick TBCs on advanced combustion. The pistons tested included:

1. A metal piston baseline at a CR of 15.8
2. A metal piston baseline at a CR of 14
3. A 1mm TBC piston at a CR of 14.7 with a dense sealing layer applied to the surface of the coating
4. A 2mm TBC piston at CR of 15.0 without dense sealing layer applied to the top surface of the coating
5. A 2mm TBC piston with CR of 15.2 with a dense sealing layer applied to the surface of the coating

A specialized injector with a 60° included angle was used to enhance the interactions between the spray and the coated piston surface and wet ethanol was used as the fuel due to its high latent heat of vaporization which can be used to counteract the charge heating of the hot piston surface associated with the thick TBC. The fuel was autoignited in HCCI as a representative advanced combustion strategy. The following conclusions can be obtained from the study.

The effects of thick TBCs on combustion and performances are as follows:

1. Thick TBC may slightly increase the PPRR and lower the burn duration. However, generally, no significant impacts on the heat release rate were observed.
2. Thick TBCs increase combustion efficiency and the level of increase is related to the thickness of the coating
3. TBCs can increase thermal efficiency by reducing the heat transfer losses from the engine cycle. Similar to the above, the increase in thermal efficiency is related to the thickness of the coating.
4. A dense sealing layer applied to the top of the TBC reduces the UHC emissions and improves combustion efficiency.
5. The combined effect of the increase in combustion efficiency and thermal efficiency is that the fuel conversion efficiency of a coated, sealed piston can be significantly higher than a metal piston in advanced combustion concepts.
6. Thick TBCs can reduce the intake temperature requirement for high latent heat vaporization fuels, such as wet ethanol.

References

[1]. Dec, John E. "Advanced compression-ignition engines—understanding the in-cylinder processes." Proceedings of the combustion institute 32, no. 2 (2009): 2727-2742.

[2]. Reitz, Rolf D. "Directions in internal combustion engine research." Combustion and Flame 1, no. 160 (2013): 1-8.

[3]. Heywood, John B. Internal Combustion Engine Fundamentals. New York: McGraw-Hill Education, 2018.

[4]. Thring, Robert H. Homogeneous-charge compression-ignition (HCCI) engines. No. 892068. SAE Technical paper, 1989.

[5]. Eng, J.A., 2002. Characterization of pressure waves in HCCI combustion (No. 2002-01-2859). SAE Technical Paper.

[6]. Saxena, Samveg, and Iván D. Bedoya. "Fundamental phenomena affecting low temperature combustion and HCCI engines, high load limits and strategies for extending these limits." Progress in Energy and Combustion Science 39, no. 5 (2013): 457-488.

[7]. Rose, K. D., J. Ariztegui, R. F. Cracknell, T. Dubois, H. D. C. Hamje, L. Pellegrini, D. J. Rickeard, B. Heuser, T. Schnorbus, and A. F. Kolbeck. Exploring a gasoline compression ignition (GCI) engine concept. No. 2013-01-0911. SAE Technical Paper, 2013.

[8]. Sellnau, Mark, Matthew Foster, Kevin Hoyer, Wayne Moore, James Sinnamon, and Harry Husted. "Development of a gasoline direct injection compression ignition (GDCI) engine." SAE International Journal of Engines 7, no. 2 (2014): 835-851.

[9]. Dec, J., Yang, Y., and Dronniou, N., "Boosted HCCI - Controlling Pressure-Rise Rates for Performance Improvements using Partial Fuel Stratification with Conventional Gasoline," SAE Int. J. Engines 4(1):1169-1189, 2011, https://doi.org/10.4271/2011-01-0897.

[10]. Yan, Z., Gainey B., Hariharan D., and Lawler, B. " Improving the controllability of PFS at low boost levels by applying a Double Late Injection (DLI) strategy." International Journal of Engine Research (2019): under review.

[11]. Reitz, Rolf D., and Ganesh Duraisamy. "Review of high efficiency and clean reactivity controlled compression ignition (RCCI) combustion in internal combustion engines." Progress in Energy and Combustion Science 46 (2015): 12-71.

[12]. Dempsey, Adam B., Scott Curran, and Rolf D. Reitz. "Characterization of reactivity controlled compression ignition (RCCI) using premixed gasoline and direct-injected gasoline with a cetane improver on a multi-cylinder engine." SAE International Journal of Engines 8, no. 2 (2015): 859-877.

[13]. Lawler, Benjamin, Derek Splitter, James Szybist, and Brian Kaul. "Thermally Stratified Compression Ignition: A new advanced low temperature combustion mode with load flexibility." Applied energy 189 (2017): 122-132.

[14]. Gainey, B., Yan, Z., Gohn, J., Rahimi Boldaji, M. et al., "TSCI with Wet Ethanol: An Investigation of the Effects of Injection Strategy on a Diesel Engine Architecture," SAE Technical Paper 2019-01-1146, 2019, https://doi.org/10.4271/2019-01-1146.

[15]. Dec, J. and Sjöberg, M., "A Parametric Study of HCCI Combustion - the Sources of Emissions at Low Loads and the Effects of GDI Fuel Injection," SAE Technical Paper 2003-01-0752, 2003, https://doi.org/10.4271/2003-01-0752.

[16]. Flowers, D., Aceves, S., Martinez-Frias, J., Smith, J. et al., "Operation of a Four-Cylinder 1.9L Propane Fueled Homogeneous Charge Compression Ignition Engine: Basic Operating Characteristics and Cylinder-to-Cylinder Effects," SAE Technical Paper 2001-01-1895, 2001, https://doi.org/10.4271/2001-01-1895.

[17]. Yan, Z., Gainey, B., Hariharan, D., and Lawler, B., "Investigation into reactivity separation between direct injected and premixed fuels in RCCI combustion mode," In ASME 2019 Internal Combustion Engine Division Fall Technical Conference, ICEF2019-7130.

[18]. Gainey, B., Yan, Z., Hariharan, D., and Lawler, B., "On the Effects of Injection Strategy, EGR, and Intake Boost on TSCI with wet Ethanol," In ASME 2019 Internal Combustion Engine Division Fall Technical Conference, ICEF2019-7164.

[19]. Dec, J., Yang, Y., Dernotte, J., and Ji, C., "Effects of Gasoline Reactivity and Ethanol Content on Boosted, Premixed and Partially Stratified Low-Temperature Gasoline Combustion (LTGC)," *SAE Int. J. Engines* 8(3):935-955, 2015, https://doi.org/10.4271/2015-01-0813.

[20]. Aceves, S., Flowers, D., Espinosa-Loza, F., Martinez-Frias, J. et al., "Spatial Analysis of Emissions Sources for HCCI Combustion at Low Loads Using a Multi-Zone Model," SAE Technical Paper 2004-01-1910, 2004, https://doi.org/10.4271/2004-01-1910.

[21]. Kamo, R. and Bryzik, W., "Adiabatic Turbocompound Engine Performance Prediction," SAE Technical Paper 780068, 1978, https://doi.org/10.4271/780068.

[22]. Sudhakar, V., "Performance Analysis of Adiabatic Engine," SAE Technical Paper 840431, 1984, https://doi.org/10.4271/840431.

[23]. Kamo, R. and Bryzik, W., "Cummins/TACOM Advanced Adiabatic Engine," SAE Technical Paper 840428, 1984, https://doi.org/10.4271/840428.

[24]. Wong, V., Bauer, W., Kamo, R., Bryzik, W. et al., "Assessment of Thin Thermal Barrier Coatings for I.C. Engines," SAE Technical Paper 950980, 1995, https://doi.org/10.4271/950980.

[25]. Kosaka, H., Wakisaka, Y., Nomura, Y., Hotta, Y. et al., "Concept of "Temperature Swing Heat Insulation" in Combustion Chamber Walls, and Appropriate Thermo-Physical Properties for Heat Insulation Coat," SAE Int. J. Engines 6(1):142-149, 2013, https://doi.org/10.4271/2013-01-0274.

[26]. Moser, S.," Experimental Investigation of Low Cost, Low Thermal Conductivity Thermal Barrier Coating on HCCI Combustion, Efficiency, and Emissions," SAE WCX 2020- under review

[27]. Assanis, D. and Mathur, T., "The Effect of Thin Ceramic Coatings on Spark-Ignition Engine Performance," SAE Technical Paper 900903, 1990, https://doi.org/10.4271/900903.

[28]. Powell, Tommy, Ryan O'Donnell, Mark Hoffman, and Zoran Filipi. "Impact of a yttria-stabilized zirconia thermal barrier coating on hcci engine combustion, emissions, and efficiency." Journal of Engineering for Gas Turbines and Power 139, no. 11 (2017): 111504.

[29]. Hoffman, Mark A., Benjamin J. Lawler, Orgun A. Güralp, Paul M. Najt, and Zoran S. Filipi. "The impact of a magnesium zirconate thermal barrier coating on homogeneous charge compression ignition operational variability and the formation of combustion chamber deposits." International Journal of Engine Research 16, no. 8 (2015): 968-981.

[30]. Gainey, B., Gohn, J., Yan, Z., Malik, K. et al., "HCCI with Wet Ethanol: Investigating the Charge Cooling Effect of a High Latent Heat of Vaporization Fuel in LTC," SAE Technical Paper 2019-24-0024, 2019.

[31]. Farrell, Alexander E., Richard J. Plevin, Brian T. Turner, Andrew D. Jones, Michael O'hare, and Daniel M. Kammen. "Ethanol can contribute to energy and environmental goals." Science 311, no. 5760 (2006): 506-508.

[32]. Saffy, Howard A., William F. Northrop, David B. Kittelson, and Adam M. Boies. "Energy, carbon dioxide and water use implications of hydrous ethanol production." Energy conversion and management 105 (2015): 900-907.

[33]. Flowers, D., Aceves, S., and Frias, J., "Improving Ethanol Life Cycle Energy Efficiency by Direct Utilization of Wet Ethanol in HCCI Engines," SAE Technical Paper 2007-01-1867, 2007, https://doi.org/10.4271/2007-01-1867.

[34]. Benajes, Jesús, Antonio García, José Manuel Pastor, and Javier Monsalve-Serrano. "Effects of piston bowl geometry on Reactivity Controlled Compression Ignition heat transfer and combustion losses at different engine loads." Energy 98 (2016): 64-77.

[35]. Gainey, Brian, Deivanayagam Hariharan, Ziming Yan, Steven Zilg, Mozhgan Rahimi Boldaji, and Benjamin Lawler. "A split injection of wet ethanol to enable thermally stratified compression ignition." International Journal of Engine Research (2018): 1468087418810587.

[36]. Srinivasan, V., M. Friis, A. Vaidya, T. Streibl, and S. Sampath. "Particle injection in direct current air plasma spray: Salient observations and optimization strategies." Plasma Chemistry and Plasma Processing 27, no. 5 (2007): 609-623.

[37]. Vaidya, A., V. Srinivasan, T. Streibl, M. Friis, W. Chi, and S. Sampath. "Process maps for plasma spraying of yttria-stabilized zirconia: An integrated approach to design, optimization and reliability." Materials Science and Engineering: A 497, no. 1-2 (2008): 239-253.

[38]. Beardsley, M. Brad, Darrell Socie, Ed Redja, and Christopher Berndt. Thick Thermal Barrier Coatings (TTBCs) for Low Emission, High Efficiency Diesel Engine Components. No. DOE/OR/22580-1. Caterpillar Inc., PO Box 1875, Peoria, IL 61656-1875, 2006.
[39]. Hutchinson, J. W., and A. G. Evans. "On the delamination of thermal barrier coatings in a thermal gradient." Surface and Coatings Technology 149, no. 2-3 (2002): 179-184.
[40]. Sampath, S., W. C. Smith, T. J. Jewett, and Hwan Kim. "Synthesis and characterization of grading profiles in plasma sprayed NiCrAlY-zirconia FGMs." In Materials science forum, vol. 308, pp. 383-388. Trans Tech Publications, 1999.
[41]. Finot, M., S. Suresh, C. Bull, and S. Sampath. "Curvature changes during thermal cycling of a compositionally graded Ni□ Al2O3 multi-layered material." Materials
[42]. Dec, J., Dernotte, J., and Ji, C., "Increasing the Load Range, Load-to-Boost Ratio, and Efficiency of Low-Temperature Gasoline Combustion (LTGC) Engines," SAE Int. J. Engines 10(3):1256-1274, 2017, https://doi.org/10.4271/2017-01-0731. Science and Engineering: A 205, no. 1-2 (1996): 59-71.
[43]. Tree, D., Wiczynski, P., and Yonushonis, T., "Experimental Results on the Effect of Piston Surface Roughness and Porosity on Diesel Engine Combustion," SAE Technical Paper 960036, 1996, https://doi.org/10.4271/960036 -Effects of Engine Variables," SAE Technical Paper 2004-01-1971, 2004, https://doi.org/10.4271/2004-01-1971.

Contact Information

Ziming Yan
zimingy@clemson.edu

Definitions/Abbreviations

aTDC	after top dead center
APS	atmospheric plasma spray
CAD	crank angle degree
CA50	crank angle of 50% mass fraction burned
CCD	combustion chamber deposit
CDC	conventional diesel combustion
CO	carbon monoxide
COV	coefficient of variation
CR	compression ratio
CTE	coefficient of thermal expansion
DI	direct injected
EGR	external-cooled exhaust gas recirculation
GHRR	gross heat release rate
HCCI	homogeneous charge compression ignition
HOF	latent heat of vaporization
$IMEP_n$	net indicated effective mean pressure
IVO	intake valve open
LTC	low-temperature combustion
LTHR	low temperature heat release
MFB	mass fraction burned
NHRR	net heat release rate
NO_x	nitrogen oxides
OEM	original equipment manufacturer
OHC	oxygenated hydrocarbon
PPRR	peak pressure rise rate
RCCI	reactivity-controlled compression ignition
SOI	start of injection
SI	spark ignition
TBCs	thermal barrier coatings
TSCI	thermally stratified compression ignition
ULSD	ultra-low sulfur diesel
UHC	unburned hydrocarbon
YSZ	yttria-stabilized zirconia

Appendix

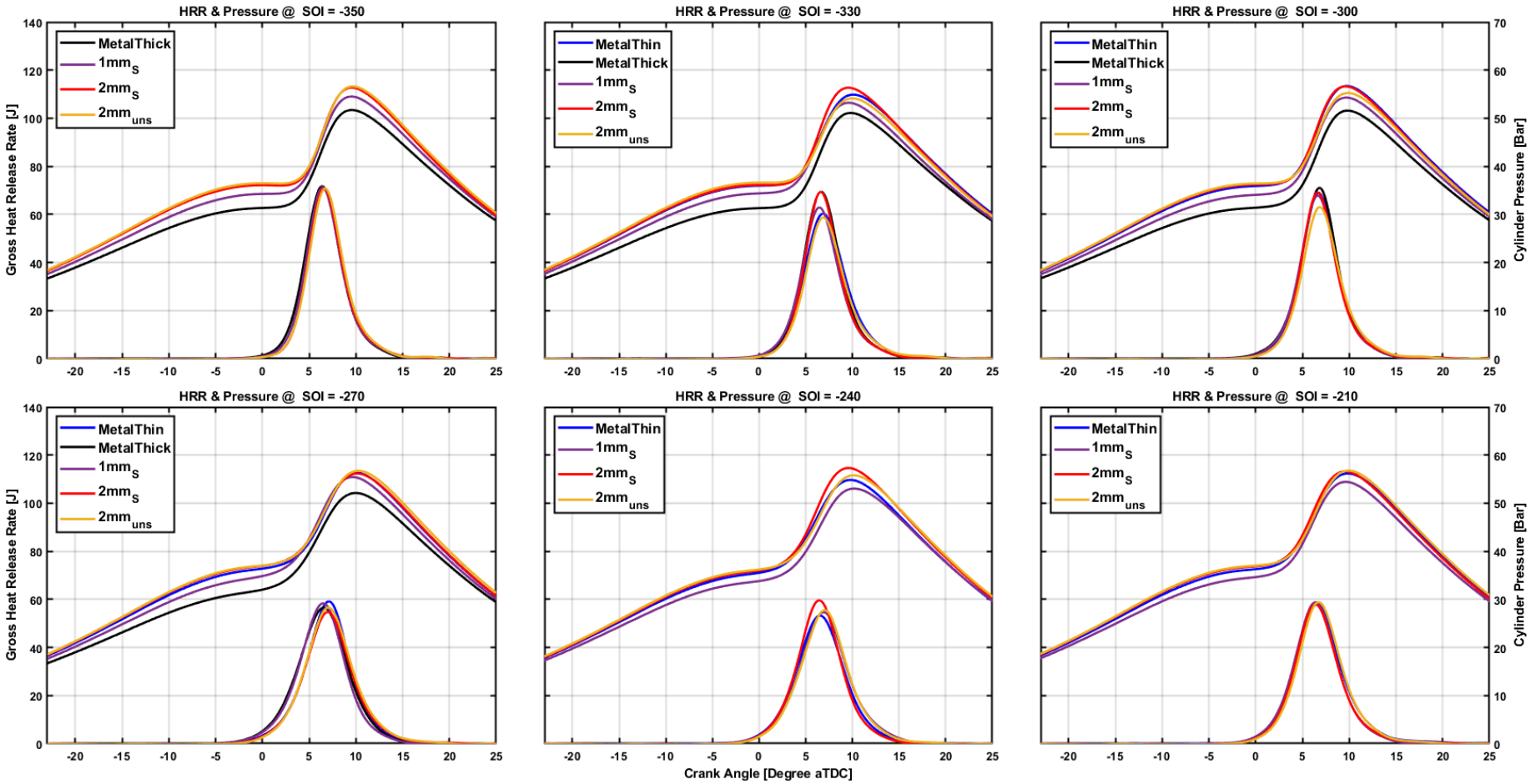

Figure 14: Gross heat release rate (bottom) & pressure trace (top) vs. crank angle degree at different SOI timings